Vesna Raspudić[1*], *Amir Ćoralić*[1], *Mersida Manjgo*[2]

INFLUENCE OF OVERFLOW TAB ON FIBRE ORIENTATION TENSOR AT WELD LINE FORMED BY INJECTION MOULDING - A NUMERICAL APPROACH

UTICAJ PRELIVNE PLOČICE NA TENZOR ORIJENTACIJE VLAKANA NA LINIJI SPAJANJA FORMIRANOJ UBRIZGAVANJEM - NUMERIČKI PRISTUP

Originalni naučni rad / Original scientific paper
Rad primljen / Paper received: 17.12.2025
https://doi.org/10.69644/ ivk-2026-01-0009

Adresa autora / Author's address:
[1)] University of Mostar, Faculty of Mechanical Engineering, Computing and Electrical Engineering, Mostar, Federation of Bosnia and Herzegovina V. Raspudić https://orcid.org/0009-0002-1787-4591
[*]email: vesna.raspudic@fsre.sum.ba
[2)] University 'Džemal Bijedić' Mostar, Faculty of Mechanical Engineering, Mostar, Federation of Bosnia and Herzegovina M. Manjgo https://orcid.org/0009-0001-1117-2620

Keywords
- polymer composites
- short fibres
- weld line
- fibre orientation tensor
- numerical simulation

Ključne reči
- polimerni kompoziti
- kratka vlakna
- linija spajanja
- tenzor orijentacije vlakana
- numerička simulacija

Abstract

The mechanical performance of a product manufactured by injection moulding depends largely on the presence of weld lines, whose occurrence is often inevitable during a production cycle. Due to poor material bonding, the weld line shows loss of strength and impact resistance under the influence of external loads, threatening the overall integrity of the product. These negative effects are particularly pronounced in short fibre reinforced composites, because there is also a local non-uniform fibre orientation. One way to mitigate these effects is to use an overflow tab, in order to create the underflow through the core material layer after the weld line is initially formed. In recent years, due to the extremely complex behaviour of short fibre reinforced composites during injection moulding, the application of numerical simulation to describe these phenomena has gained great importance. The paper presents the application of Moldex3D Studio software to predict the influence of the overflow tab on the localised reduction of mechanical properties at weld lines. This involves describing changes in the distribution of fibre orientation tensor components as well as changes in the position and shape of the weld line region.

Izvod

Mehaničko ponašanje proizvoda izrađenog brizganjem u velikoj meri zavisi od prisustva linija spajanja, čija je pojava često neizbežna tokom proizvodnog ciklusa. Zbog lošeg spajanja materijala, na liniji spajanja dolazi do gubitka čvrstoće i otpornosti na udar pod uticajem spoljašnjih opterećenja, što ugrožava sveukupni integritet proizvoda. Ovakvi negativni efekti su posebno izraženi kod kompozita ojačanih kratkim vlaknima, jer u tom slučaju postoji i lokalna neujednačenost u orijentaciji vlakana. Jedan od načina za ublažavanje ovih efekata je upotreba prelivne pločice, kako bi se stvorio povratni tok materijala kroz sloj jezgra nakon početnog formiranja linije spajanja. Poslednjih godina, zbog izuzetno složenog ponašanja kompozita ojačanih kratkim vlaknima tokom brizganja, primena numeričke simulacije za opisivanje ovih pojava dobija veliki značaj. U radu je predstavljena primena softvera Moldex3D Studio za predviđanje uticaja prelivne pločice na lokalno smanjenje mehaničkih svojstava na linijama spajanja. Opisane su promene u raspodeli komponenata tenzora orijentacije vlakana, kao i promene u položaju i obliku područja linije spajanja.

INTRODUCTION

The most important factors influencing the performance of products made of short fibre reinforced composites (SFRCs) are the material microstructure and manufacturing process /1-3/. Mechanical properties such as stiffness and strength are much higher in the direction in which more fibres are aligned /4, 5/. In the case of injection moulded parts, the manufacturing process induces a complex, locally varying fibre orientation which significantly affects the mechanical performance of the final part. This is particularly evident in the vicinity of injection gates, as well as in the places where materials are joined from different directions forming weld lines, for example in the case when there are obstacles to the polymer flow or when there is more than one gate /6-10/.

Given the complexity of the interactions between matrix, fibres and processing conditions, it is very difficult to predict the integrity of specific products, and standardised experimental verification of such composite materials is necessary /11/. In recent years, the application of numerical simulation of injection moulding process has also become increasingly important /12-14/. The results of CAE (Computer Aided Engineering) analysis provide insight into the causes of problems that may arise and enable the testing of different solutions to find the most suitable one. This cannot be achieved with the traditional experimental trial-and-error approach, as this requires a significant investment of time and material resources. In contrast, CAE offers the possibility of iteratively testing different solutions to achieve suitable or even optimal process parameters and design geometry.

WELD LINES

Based on how they develop, the weld lines can be classified into two different categories: weld lines formed by opposite flow fronts (head-on collision) and weld lines formed by side flow fronts. The localised reduction of mechanical properties, i.e., loss of strength and impact resistance, is particularly pronounced in the case of the head-on collision. This is the result of the so-called 'fountain flow' during the filling phase, represented in Fig. 1.

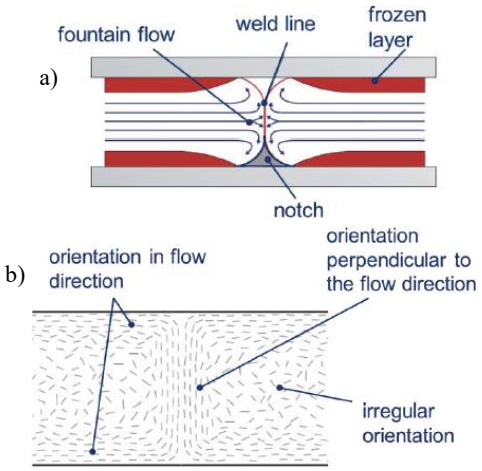

Figure 1. a) Fountain flow of the melt in the mould; b) schematic fibre orientation at the weld line, /15/.

When SFRC enters the cold mould cavity, it solidifies in contact with the cavity wall developing frozen layers or the so-called skin layers with preferential fibre orientation parallel to the flow direction due to the dominant shear deformations in that area. In the core region, the flow is more divergent, resulting in irregular fibre orientation. In the weld line region, the fibres are orientated mostly perpendicular to the flow direction, so the stresses are mostly transmitted by the intermolecular forces of the matrix material. This orientation increases the negative effects further, because it prevents the mutual diffusion of macromolecules of the matrix, which leads to an additional decrease in the strength of the weld line. In addition, there are often air traps because the air cannot escape between the melt streams. Furthermore, a crack initiation can occur on the surface of the part in the weld line region due to a V-notch which can be formed if the two melt streams freeze too fast at the mould wall /15/. All of the above increases the risk of mechanical failure in the case when a SFRC part with weld line is exposed to external loads.

It has been shown that the weld line strength for unreinforced polymers can be improved using high values of mould and melt temperature during the injection moulding process, as well as by increasing pack pressure /2, 16/. However, in the case of reinforced plastics, the fibre orientation cannot be significantly changed by modifying mould and melt temperatures. To be reoriented, reinforcement fibres need a mechanical force induced by the polymer melt flow right after the weld line formation. One of the ways to achieve this is by using overflow tab, which is offset from the weld line in order to create underflow effect through the core of the part after the weld line is initially formed, /17, 18/.

FIBRE ALIGNMENT PREDICTION

The orientation of a single rigid cylindrical fibre in a three-dimensional space can be described by unit vector $\mathbf{p}(\varphi, \theta)$ directed along the fibre axis, as shown in Fig. 2,

$$\mathbf{p} = \begin{Bmatrix} p_1 \\ p_2 \\ p_3 \end{Bmatrix} = \begin{Bmatrix} \cos\varphi \sin\theta \\ \sin\varphi \sin\theta \\ \cos\theta \end{Bmatrix}. \tag{1}$$

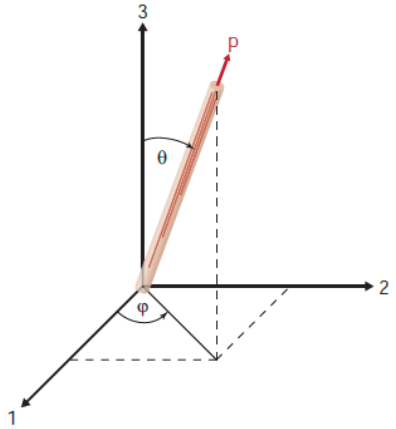

Figure 2. The orientation of a single rigid cylindrical fibre, /19/.

Even in a small volume, adjacent fibres are not aligned in the same direction and have a distinct orientation distribution instead. The orientation state of a group of fibres in a defined volume can be described by a probability density distribution function $\psi(\mathbf{p})$, which describes the probability of a fibre to be oriented between angles θ_i and $(\theta_i + d\theta)$, and between φ_i and $(\varphi_i + d\varphi)$.

The conventional representation in the field of discontinuous fibre-reinforced composites is the Advani-Tucker orientation tensor which considers an average orientation property of all fibres within a discrete volume, /20/:

$$\mathbf{A} = \oint \psi(\mathbf{p}) \mathbf{p}\mathbf{p} d\mathbf{p} = \begin{bmatrix} A_{11} & A_{12} & A_{13} \\ A_{12} & A_{22} & A_{23} \\ A_{13} & A_{23} & A_{33} \end{bmatrix}. \tag{2}$$

The volume is assumed to be large enough to contain sufficient fibres and still small enough to ensure a uniform orientation distribution of fibres within the volume. The fibre orientation tensor **A** is a symmetric positive semidefinite 3 × 3 tensor with the trace, i.e., the sum of elements on its main diagonal:

$$tr(\mathbf{A}) = \sum_{i=1}^{3} A_{ii} = A_{11} + A_{22} + A_{33} = 1, \tag{3}$$

and represents a compact measure of fibre orientation distribution in volume V. The diagonal components of the orientation tensor (A_{11}, A_{22} and A_{33}) describe the degree of orientation with respect to the defined coordinate system. Conventionally, the reference coordinates are defined so that the 1-direction represents the in-flow direction, the 2-direction is the cross-flow direction, and the 3-direction is the thickness direction. The off-diagonal components of the orientation tensor show the tilt of the orientation tensor from the coordinate axes. Hence, they are zero only if the coordinate axes align with principal directions of the orientation tensor.

The physical interpretation of tensor components focuses mainly on the diagonal components of the tensor, illustrated in Fig. 3. A completely random orientation (left in Fig. 3) can be described by diagonal components $A_{11} = A_{22} = A_{33} = 1/3 = 0.33$. Perfectly aligned fibres, for example in the 1-direction (right in Fig. 3), can be described by $A_{11} = 1$, $A_{22} = A_{33} = 0$.

A is the principal quantity of interest for commercial injection moulding simulations as it may vary for every Gauss point of the FEM mesh, /21/.

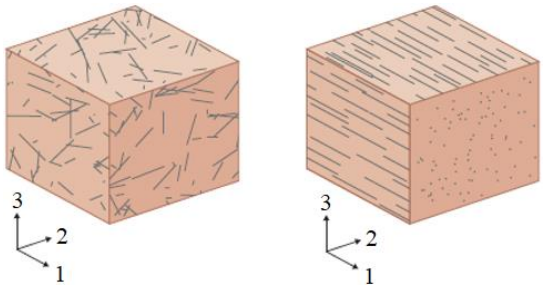

Figure 3. Physical interpretation of the tensor components, /19/.

Over the last three decades, a few representative theoretical models for fibre alignment prediction have been developed, /22/. Modern fibre orientation models, based on classic fibre orientation models, the Jeffery hydrodynamic (HD) model and the Folgar-Tucker isotropic rotary diffusion (IRD) model, include the Phelps-Tucker anisotropic rotary diffusion (ARD) model, the Wang-Tucker reduced strain closure (RSC) model, and the ARD-RSC model. Following these fibre orientation models, Tseng et al. further developed the improved iARD-RPR model.

Macroscopic fibre orientation models are computationally efficient and are implemented in commercial injection moulding software for estimating fibre orientation in large industrial applications. For example, Moldex3D provides the Folgar-Tucker, ARD and iARD-RPR models. The limitation of these models is their dependency on a set of fitting parameters that need to be selected to obtain an accurate orientation prediction. For example, the iARD-RPR model has three physical parameters: a fibre-fibre interaction parameter C_I, a fibre matrix interaction parameter C_M and a slow-down parameter α. The available region of these parameters is: $0 < C_I < 0.1$, $0 < C_M < 1$, and $0 < \alpha < 1$. Thereby, the shell-orientation layer depends on iARD parameters, while the core width is controlled by the RPR parameter, /23/. The value of fibre orientation in the shell increases with increasing C_I and decreasing C_M. The core width increases with increasing α. According to these criteria, an optimal parameter set for a given problem can be defined in order to get an accurate orientation prediction verified with experimental data, for example, measured by micro-computed tomography (micro-CT).

NUMERICAL SIMULATION

In this study, we used Moldex3D Studio to simulate the effect of overflow tab on fibre orientation tensor by using the geometry of tensile test specimens, according to ISO 527 type 1B /24/, with the length of narrow parallel-sided portion of $l_1 = 60$ mm, width at narrow portion $b_1 = 10$ mm and specimen thickness of $h = 4$ mm (Fig. 4).

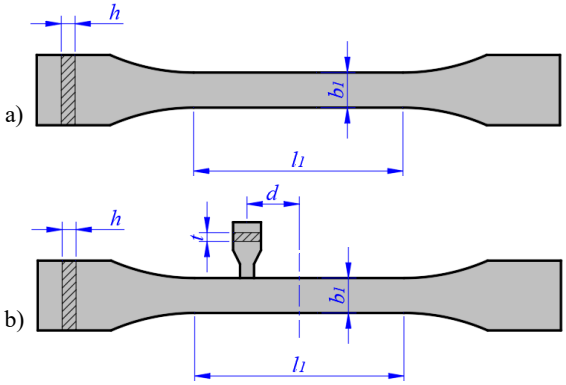

Figure 4. Geometry of the tensile test specimen according to ISO 527, type 1B: a) without overflow tab; b) with overflow tab.

Five different configurations are observed: the model with one gate (M1), the model with two identical gates at opposite ends (M2), and the model with two identical gates at opposite ends and an overflow tab offset from the specimen centre at distances d of 5 mm, 15 mm and 25 mm (M2-5, M2-15 and M2-25) (Fig. 5).

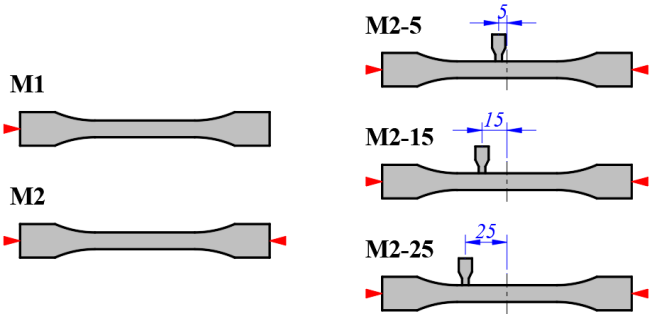

Figure 5. Simulation models.

To create the underflow effect, the overflow tab dimensions are designed to be completely filled after forming of the weld line in the basic specimen geometry. In order to cause the hesitation effect, the overflow tab thickness should be less than the specimen thickness and here it is set to $t = 2.5$ mm.

In all simulations, selected material is the commercial composite with glass fibre concentration of 40 wt.% and matrix resin of polyamide 6 (PA6), grade name Akulon K224-G8, produced by DSM Engineering Plastics /25/. The fibre orientation was predicted by the iARD-RPR model, using the parameters: $C_I = 0.005$, $C_M = 0$ and $\alpha = 0.7$.

The process parameters are taken in accordance with Moldex3D Studio recommendations for the considered material and the geometry of specimens: the filling time 0.4 s, mould temperature 65 °C and melting temperature 265 °C.

The chosen mesh for the simulation is solid with 11 layers of boundary layer mesh (BLM), and an automatic boundary layer offset ratio (Fig. 6). BLM allows generating of injection flow of multiple layers with prismatic elements created out of triangular surface mesh. The internal space is filled with tetrahedral mesh. The mesh seed size is set to 0.5.

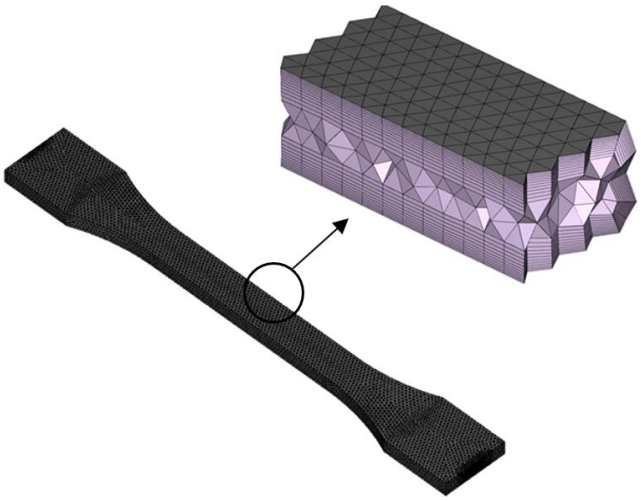

Figure 6. 11-layer boundary layer mesh (BLM).

RESULTS AND DISCUSSION

Figures 7 and 8 show the distribution of tensor components A11 (flow direction), A22 (crossflow direction) and A33 (thickness direction) obtained for specimens with one gate (M1), i.e., with two gates without overflow tab (M2). The distribution is measured at the centre of the specimen across its thickness.

It is evident that the fibre orientation differs significantly with the formation of the weld line. In both configurations, the thickness distribution can be described by the five-layer structure: two skin layers (at the surface of the specimen, 0-5 % and 95-100 % of the relative thickness), one core layer (in the middle of the specimen, 35-65 % of the relative thickness) and two shell layers (between skin and core layer, 5-35 % and 65-95 % of relative thickness). In the case of the one-gated M1 configuration, the high rate of A11, especially in the shell layers, with values in the range from 0.80 to 0.85, indicates that most fibres are oriented in the flow direction. In the case of model M2, the values of A11 at the location of the weld line are low (≈ 0.1), since fibres are oriented mostly in transverse directions.

The complete region where the formation of the weld line will lead to a severe deterioration of mechanical properties in the longitudinal direction (with A11 < 0.33) can be seen in Fig. 9.

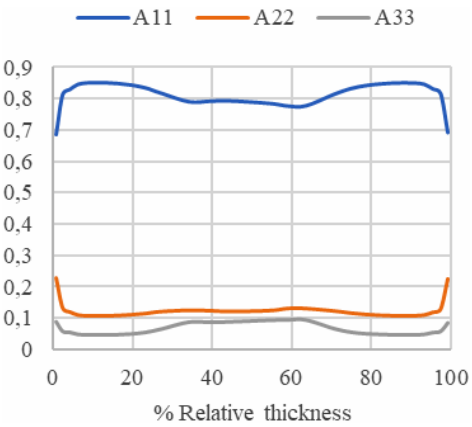

Figure 7. Fiber orientation distribution for model M1 (one-gated specimen without overflow tab) at the centre of specimen.

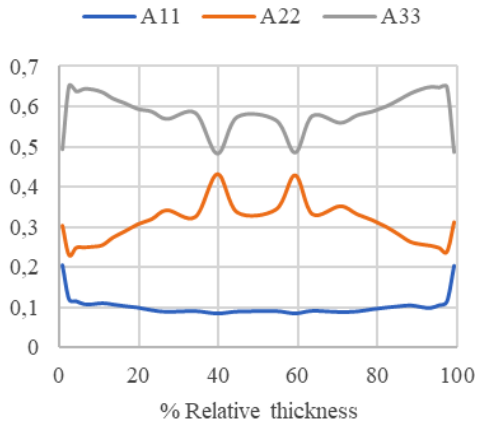

Figure 8. Fiber orientation distribution for model M2 (two-gated specimen without overflow tab) at the centre of specimen.

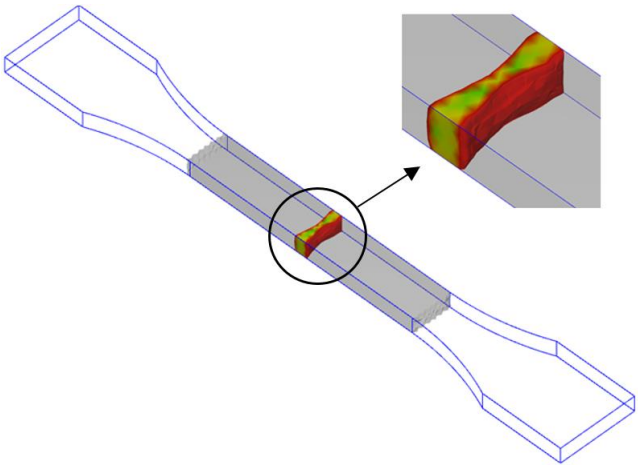

Figure 9. Weld line region with A11 < 0.33 for model M2.

Figure 10 shows the results for fibre thickness distribution at the weld line for the model with the overflow tab set at distance of 5 mm from specimen centre (model M2-5).

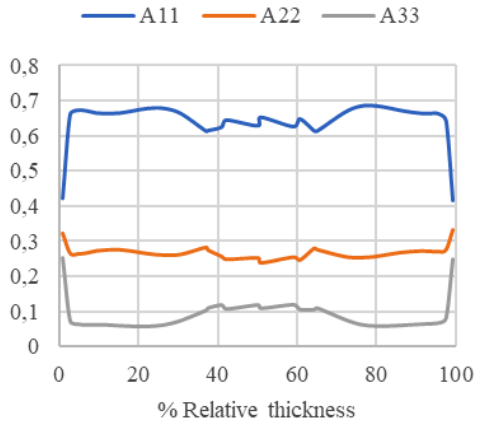

Figure 10. Fiber orientation distribution for model M2-5 (two-gated specimen with overflow tab) at the weld line.

As it can be seen, due to the overflow effect there is an improvement in the distribution of fibres in the flow direction at the weld line, which in this case nearly coincides with the central line of the specimen (Fig. 11).

However, when using the overflow tab, the change in the melt flow direction at the entrance into the tab creates a poor area with regard to fibre orientation in the flow direction. In this case, with the tab very slightly displaced from the spec-

imen centre, the region with extremely low A11 values (< 0.33) extends almost over the entire cross-section area of the specimen (Figs. 12 and 13). Therefore, this position of the tab does not contribute to a significant improvement in fibre distribution, since the bad region is essentially shifted from the location of the weld line to the location of the tab placement.

In this case, the weld line is shifted by 0.85 mm relative to the centre of specimen (Fig. 14).

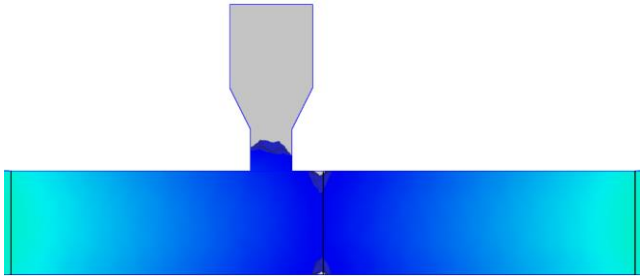

Figure 11. Filling of the model M2-5 at 96 % of the filling time.

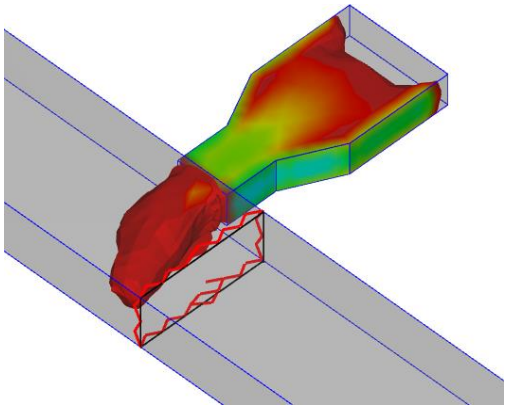

Figure 12. Region with A11 < 0.33 for model M2-5 at the end of filling time, isometric view.

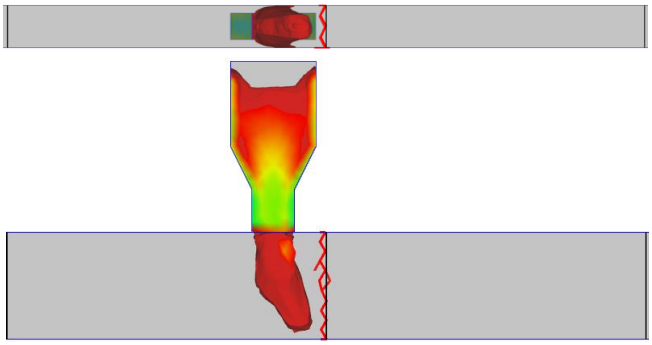

Figure 13. Region with A11 < 0.33 for model M2-5 at the end of filling time, frontal and top view.

Figure 15 shows the thickness distribution curves at the weld line for specimen with the overflow tab set at distance of 15 mm from specimen centre (model M2-15). As it can be seen, the fibre orientation distribution in the flow direction at the weld line is now much better compared to the two-gated specimen without the overflow tab (model M2, Fig. 8).

The poor area with low values of the A11 component due to the change in flow direction is also significantly smaller compared to the M2-5 model and does not extend across the entire specimen cross-section (Figs. 16 and 17).

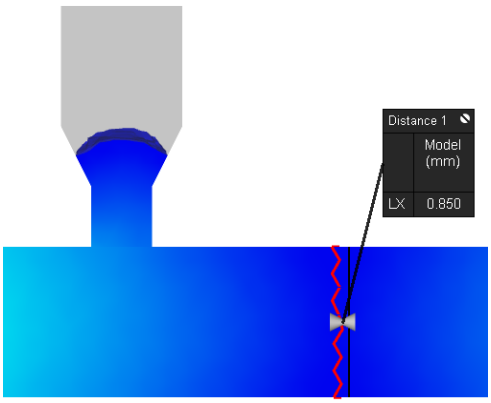

Figure 14. Filling of the model M2-15 at 96.5 % of filling time.

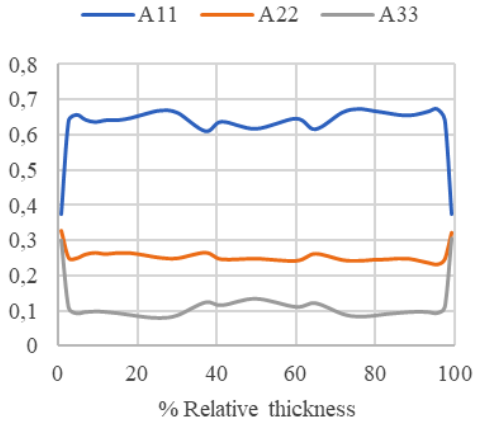

Figure 15. Fiber orientation distribution for model M2-15 (two-gated specimen with overflow tab) at the weld line.

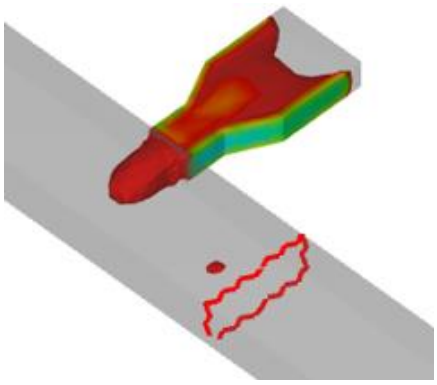

Figure 16. Region with A11 < 0.33 for model M2-15 at the end of filling time, isometric view.

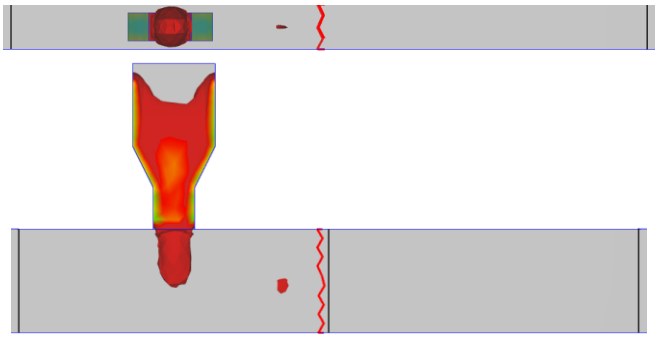

Figure 17. Region with A11 < 0.33 for model M2-15 at the end of filling time, frontal and top view.

The fibre orientation distribution at the weld line for the specimen with overflow tab set at distance of 25 mm from the specimen centre (model M2-15) is given in Fig. 18 with A11 values significantly lower than in the two preceding models with overflow tabs (M2-5 and M2-15), especially in the core layer. This can be explained by the fact that the tab is already mostly filled by the time the weld line is formed in the specimen, so that the appropriate overflow effect cannot be achieved (Fig. 19). The weld line in this case is shifted at a distance 1.5 mm from the specimen centre.

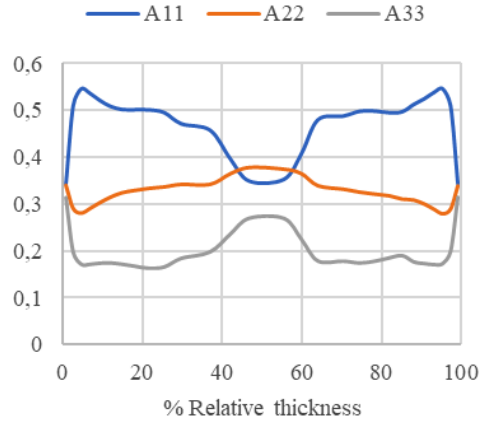

Figure 18. Fibre orientation distribution for model M2-25 (two-gated specimen with overflow tab) at the weld line.

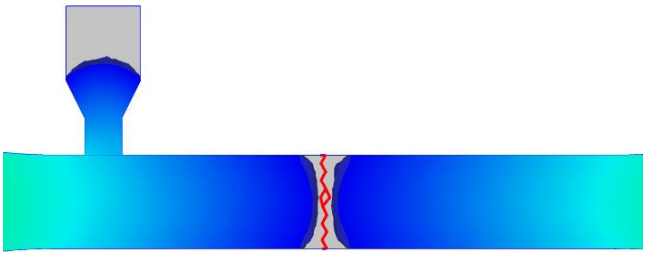

Figure 19. Filling of the model M2-25 at 96 % of filling time.

It is also interesting to notice that the planar weld line region, as it exists in the case of a specimen without an overflow tab (model M2), now takes on a parabolic shape (Figs. 20 and 21).

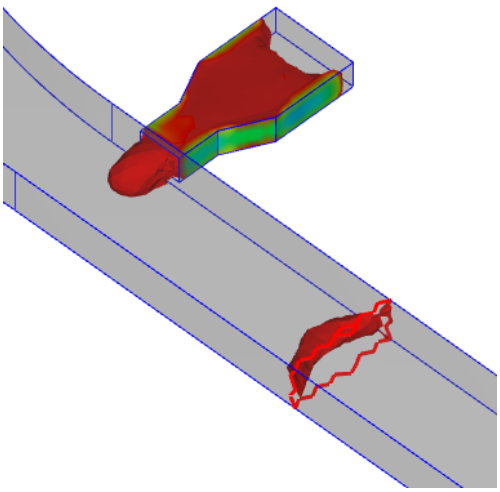

Figure 20. The region with A11 < 0.33 for the model M2-25 at the end of filling time, isometric view.

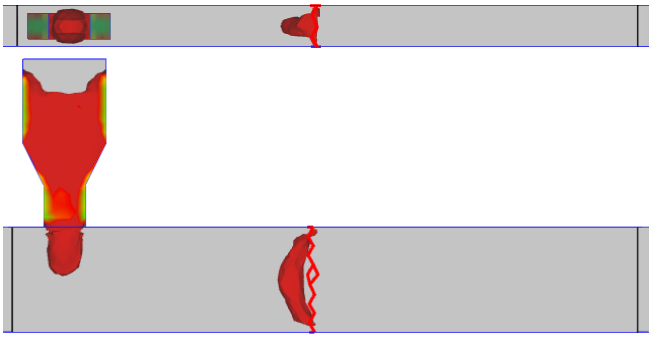

Figure 21. Region with A11 < 0.33 for model M2-25 at the end of filling time, frontal and top view.

CONCLUSION

The paper presents the results of a numerical analysis whose goal is to predict the influence of the overflow tab on the position and quality of the weld line formed by injection moulding of the tensile test specimen with two gates. It has been shown that proper tab positioning can significantly contribute to the quality of the fibre orientation tensor at the weld line region. If the tab is placed too close to the weld line position, the change in flow direction will cause a bad area with low values of fibre orientation tensor in the flow direction that extends over a large part of the cross-section of the specimen. On the contrary, in the case when the tab is located too far away, it is not possible to achieve the appropriate overflow effect, whereby the change in the shape of the weld line region occurs, i.e., it comes to its transition from the originally planar to a parabolic shape. The M2-15 model shows a significant improvement in fibre orientation compared to the model without a tab, which confirms the justification of its application in cases where the formation of a weld line can violate the integrity of the product. Based on the appropriate position and alignment of the overflow tab determined by numerical simulation, experimental tests can provide additional confirmation of the accuracy of the parameters used in the iARD-RPR model.

ACKNOWLEDGEMENTS

This paper is published as a part of the scientific research project ‘Optimisation of the weld line configuration on elements made of injection-moulded polymer composite materials,’ 05-35-4537-1/24, supported by the Federal Ministry of Education and Science, Federation of Bosnia and Herzegovina.

Authors would like to express their gratitude to company CORETECH System Co., Ltd. for their support related to numerical simulations and granting access to Moldex3D Studio software.

REFERENCES

1. Crawford, R.J., Martin, P.J., Plastics Engineering, Academic Press, Elsevier: Butterworth-Heinemann, 2020.
2. Erhard, G., Designing with Plastics, Carl Hanser Verlag, Munich, 2006.
3. Baur, E, Osswald, T.A., Rudolph, N., Plastics Handbook, The Resource for Plastics Engineers, 5th Ed., Carl Hanser Verlag, Munich, 2019.

4. Fu, S., Lauke, B., Mai, Y.-W., Science and Engineering of Short Fibre-Reinforced Polymer Composites, Woodhead Publ., 2009.
5. Lewis, C., Yavuz, B.O., Longana, M.L., et al. (2024), *A review on the modelling of aligned discontinuous fibre composites*, J Compos. Sci. 8(8): 318. doi: 10.3390/jcs8080318
6. Huang, C.-T., Chen, X.-W., Fu, W.-W. (2020), *Investigation on the fiber orientation distributions and their influence on the mechanical property of the co-injection molding products*, Polymers, 12(1): 24. doi: 10.3390/polym12010024
7. Bociąga, E., Skoneczny, W. (2020), *Characteristics of injection molded parts with the areas of weld lines*, Polimery, 65(5): 337-345. doi: 10.14314/polimery.2020.5.1
8. Baradi, M.B., Cruz, C., Riedel, T., Régnier, G. (2019), *Frontal weld lines in injection-molded short fiber-reinforced PBT: Extensive microstructure characterization for mechanical performance evaluation*, Polym. Compos. 40(12): 4547-4558. doi: 10.1002/pc.25310
9. Kurkin, E.I., Spirina, M.O., Chertykovtseva, V.O., Zakhvatkin, Ya.V. (2020), *Mechanical characteristics of short fiber composite samples located behind circle, rectangle, triangle obstacles*, IOP Conf. Ser.: Mater. Sci. Eng. 868: 012024. doi: 10.1088/1757-899X/868/1/012024
10. Li, X-J., Zuo, Z-M., Mi, H-Y., et al. (2024), *A review of research progress on the minimization of weld lines in injection molding*, Int. J Adv. Manuf. Technol. 132(11-12): 5179-5210. doi: 10.1007/s00170-024-13607-7
11. Lazović, T., Ljubojević, P., Trišović, N., Trišović, Z. (2024), *Composite materials - current state of standardization*, Struct. Integr. Life, 24(1): 71-80. doi: 10.69644/ivk-2024-01-0071
12. https://www.moldex3d.com
13. Foss, P. H., Tseng, H.-C., Snawerdt, J., et al. (2014), *Prediction of fiber orientation distribution in injection molded parts using Moldex3D simulation*, Polym. Compos. 35(4): 671-680. doi: 10.1002/pc.22710
14. Pavia, F., Item, R., Negri, F., et al. (2021), *Structural analysis of short fiber reinforced plastics*, Tech. Paper, ANSYS Inc., 2021.
15. Geyer, A., Bonten, C. (2019), *Enhancing the weld line strength of injection molded components*, AIP Conf. Proc. 2055: 070023. doi: 10.1063/1.5084867
16. Jadhav, G., Gaval, V., Divekar, M., Darade, N. (2022), *Effect of packing pressure on stagnation weld-line strength for thermoplastic semicrystalline glass fiber reinforced material*, J Thermopl. Compos. Mater. 36(10): 3874-3890. doi: 10.1177/08927057221142244
17. Scantamburlo, A., Sorgato, M., Lucchetta, G. (2020), *Investigation of the inflow effect on weld lines morphology and strength in injection molding of short glass fiber reinforced polypropylene*, Polym. Compos. 41(7): 2634-2642. doi: 10.1002/pc.25562
18. https://www.moldex3d.com/blog/top-story/effect-of-overflow-tab-on-major-modulus-of-weld-line-in-glass-fiber-filled-injection-molded-parts
19. Gandhi, U.N., Goris, S., Osswald, T.A, Song, Y.-Y., Discontinuous Fiber-Reinforced Composites: Fundamentals and Applications, Carl Hanser Verlag, Munich, 2020. ISBN 9781569906941
20. Advani, S.G., Tucker, C.L. (1987), *The use of tensors to describe and predict fiber orientation in short fiber composites*, J Rheol. 31(8): 751-784. doi: 10.1122/1.549945
21. Köbler, J., Schneider, M., Ospald, F. et al. (2018), *Fiber orientation interpolation for the multiscale analysis of short fiber reinforced composite parts*, Comput. Mech. 61: 729-750. doi: 10.1007/s00466-017-1478-0
22. Tseng, H.-C., Chang, R.-Y., Hsu, C.-H. (2018), *Comparison of recent fiber orientation models in injection molding simulation of fiber-reinforced composites*, J Thermopl. Compos. Mater. 33(1): 35-52. doi: 10.1177/0892705718804599
23. Tseng, H.-C., Chang, R.-Y., Hsu, C.-H. (2018), *The use of shear-rate-dependent parameters to improve fiber orientation predictions for injection molded fiber composites*, Compos. Part A: Appl. Sci. Manuf. 104: 81-88. doi: 10.1016/j.compositesa.2017.10.031
24. ISO 527-2:2025, Plastics - Determination of tensile properties, Part 2: Test conditions for moulding and extrusion plastics, Ed. 3, 2025.
25. https://www.lookpolymers.com/polymer_DSM-Akulon-K224-G8-PA6-GF40.php (last accessed on March 10, 2026)